Title: Distribution of Palinuridae and Scyllaridae phyllosoma larvae within the East Australian Current: a climate change hot-spot

Authors: Laura N. Woodings[A,G], Nick P. Murphy[A], Andrew Jeffs[B], Iain M. Suthers[C], Geoffrey W. Liggins[D], Bridget S. Green[E], Jan M. Strugnell[A,F].

[A]Department of Ecology, Environment and Evolution, School of Life Sciences, La Trobe University, Bundoora, Vic. 3086, Australia.

[B]School of Biological Sciences and Institute of Marine Science, University of Auckland, Auckland 1142, New Zealand.

[C]School of Biological, Earth & Environmental Sciences, University of New South Wales, Sydney, NSW 2052, Australia.

[D]NSW Department of Primary Industries, Sydney Institute of Marine Science, Mosman NSW 2088, Australia

[E]Institute for Marine and Antarctic Studies, University of Tasmania, Hobart, Tas. 7001, Australia

[F]Centre for Sustainable Tropical Fisheries and Aquaculture and College of Science and Engineering, James Cook University, Townsville, Qld 4811, Australia.

[G]Corresponding author: Email: 17869067@students.latrobe.edu.au

Abstract

Many marine species are predicted to shift their ranges poleward due to rising ocean temperatures driven by climate change. For benthic marine species with pelagic larval stages, poleward range shifts are often facilitated through pelagic larval transport via western boundary currents (WBC). By surveying pelagic larval distributions within WBCs, species advected poleward of their known distributions can be identified and monitored. Palinurid and scyllarid lobster larvae (phyllosoma) have long pelagic larval

durations, providing high potential for poleward advection. We surveyed spatial distribution of phyllosoma within the western-boundary East Australian Current. Due to difficulties morphologically identifying phyllosoma, we tested the utility of molecular identification using cytochrome *c* oxidase I (COI). From COI sequences of 56 phyllosoma and one postlarva, 65% of sequences consisted of good-quality mitochondrial DNA. Across water types sampled, scyllarid phyllosoma exhibited relatively homogeneous distribution, whereas palinurid phyllosoma exhibited heterogeneous distribution with greatest abundance inside a warm core eddy on the south coast of eastern Australia. Two tropical and one subtropical palinurid species were detected ~75–1800 km to the south or south-west of their known species distribution. Our results indicate tropical lobster species are reaching temperate regions, providing these species the opportunity to establish in temperate regions if or when environmental conditions become amenable to settlement.

1.1 Introduction

As ocean temperatures increase due to climate change, many marine species are moving their latitudinal range poleward due to temperatures at lower latitudes exceeding the limits of their thermal tolerance (Sunday *et al*. 2012; Pinsky *et al*. 2013; Poloczanska *et al*. 2016; Pecl *et al*. 2017). Poleward range extensions for most sessile or sedentary marine benthic species is facilitated by a dispersive pelagic larval phase (Cowen and Sponaugle 2009) and is largely contingent on ocean currents (Sorte *et al*. 2018), such as western boundary currents (WBC). To date WBCs have played an important role in poleward range shifts of many marine species (Vergés *et al*. 2014). Under the influence of climate change, WBCs are warming two- to threefold faster than the global average and intensifying (Ridgway and Hill 2012; Sun *et al*. 2012; Matear *et al*. 2013), transporting larger volumes of warmer water poleward, often at higher velocities. As a result, these

areas are providing hot spots for species range shifts (Pitt *et al*. 2010; Johnson *et al*. 2011; Robinson *et al*. 2015).

The East Australian Current (EAC) is a southerly flowing WBC linked to the poleward range shifts of several marine species in recent years, such as sea urchins, octopus and numerous reef and pelagic fish (Booth *et al*. 2007; Ling *et al*. 2009; Stuart-Smith *et al*. 2018; Ramos *et al*. 2018). Although these range shifts include several species with adult mobility, they also include benthic organisms that are known to have slower range shift responses than highly mobile species (Sunday *et al*. 2015; Pecl *et al*. 2017). Planktonic studies have revealed that larval assemblages transported by the EAC and its eddies are often different to those in the surrounding waters, with a high prevalence of tropical species occurring in the warm EAC waters (Brandt 1981; McWilliam and Phillips 1983; Tranter *et al*. 1983; Lobel and Robinson 1988; Keane and Neira 2008; Syahailatua *et al*. 2011). By 2060, oceanographic simulations predict volume transport increases of 12% in the EAC core region and 35–40% in the EAC extension, with an increase in eddy field activity (Ridgway and Hill 2012; Sun *et al*. 2012; Matear *et al*. 2013). As the volume of warm water reaching higher latitudes increases, it will provide increased opportunities for pelagic larvae to be transported poleward, creating the potential for some tropical species to establish populations beyond their existing adult range, if benthic environmental conditions are favourable. Considering the first step of a range shift is arrival (Bates *et al*. 2014), identifying species advected outside their adult range provides knowledge of species with the potential to undergo the first stage of a range shift in the future.

Spiny and slipper lobsters (families Palinuridae and Scyllaridae respectively) are ubiquitous along the east Australian coast, occurring both in tropical (Queensland and northern New South Wales, NSW) and temperate (southern NSW, Victoria and Tasmania) areas. The pelagic larvae, or phyllosoma, of palinurid and scyllarid lobsters are

particularly suited to dispersal via ocean currents due to their transparent, leaf-like body shape (Booth and Phillips 1994) and their long pelagic larval phases, which range from a few months to >1 year in duration (Booth and Phillips 1994; Booth *et al*. 2005). Lobsters are of high commercial importance along the east Australian coast, with 2121 tonnes of spiny lobster and 607 tonnes of slipper lobsters being landed in the 2016–17 season (Stewardson *et al*. 2018). There is some concern of the potential recruitment and fisheries effects that could occur for native lobster species if lower-latitude lobster species range shift polewards (Pecl *et al*. 2009). Despite this, there is little empirical information on phyllosoma species assemblages and distribution within EAC waters and eddies.

Assessing phyllosoma species assemblages and distribution is difficult because phyllosoma undergo many physical changes due to multiple instar stages, making species identification through examination of morphology notoriously difficult (Chow *et al*. 2006*a*). Molecular identification through DNA barcoding has been suggested as an alternative method for identifying phyllosoma to species level (Chow *et al*. 2006*a*); however, currently there is no a gold-standard barcoding region to use for palinurid and scyllarid species, with some studies using the *16S* rRNA region (Konishi *et al*. 2006; García-Rodríguez *et al*. 2008; Genis-Armero *et al*. 2017) and others using cytochrome *c* oxidase I (*COI*; Chow *et al*. 2006*a*, 2006*b*; Canto-García *et al*. 2016). For animals *COI* is normally the barcode of choice, although for some cave and freshwater crustaceans this barcode has nuclear copies that can be highly divergent from the mitochondrial *COI* region, leading to incorrect barcode assignment (Buhay 2009). Therefore, given the importance of DNA barcoding for phyllosoma identification, and the ubiquitous use of the *COI* barcode across most animal species, empirical assessment of the utility of the *COI* barcoding region in palinurid and scyllarid lobsters is needed.

The aim of this study was to determine the mid-year spatial distribution of phyllosoma along the mid-eastern Australian coast by identifying phyllosomas to species level using DNA barcoding. First, we assessed the suitability of mitochondrial *COI* as a barcoding region for identifying a mixture of unknown phyllosoma sourced from plankton trawls. Second, we compared the phyllosoma distribution in relation to their adult distribution to gain an understanding of the species with the potential to undergo the first stage of a range shift.

1.2 Materials and methods

1.2.1 Sample collection

Phyllosoma samples were collected on board the *RV Investigator* from 3 to 18 June 2015, within the area 27°34′–34°03′S and 156°52′–152°01′E (refer to Table 1). A total of 34 stations were sampled, with either a multiple opening and closing net and environmental sensing system (MOCNESS; diameter 1 m^2, mesh 500 µm), a neuston net (surface tow net; diameter 1 m^2, mesh 500 µm) or a rectangular mid-water trawl (RMT) net (diameter 1.13 m^2, mesh = 1000 µm; Table 1). All nets were fitted with 500-µm mesh codends. Tow duration was 10 min per haul for the MOCNESS and neuston nets and 30 min per haul for the RMT net. At each sampling station, hauls from either two to four MOCNESS and two neuston nets, or three RMT nets were conducted and live sorted immediately upon landing. All phyllosoma and postlarval lobster stages found in those hauls were preserved in 70% ethanol and stored at –80°C.

1.2.2 Molecular techniques

DNA was extracted from leg and antenna tissue using a DNeasy Blood and Tissue Kit (Qiagen, Valencia, CA, USA). Universal *COI* primers (Folmer *et al*. 1994) were used for DNA barcoding. Polymerase chain reactions (PCR) were performed in a total volume of 12.5 µL, consisting of 1× MyTaq Red Mix (Bioline, London, UK), 0.2 µM of each

primer, 1.5 mM $MgCl_2$ and 32–140 ng of DNA. The PCR thermal cycle consisted of an initial denaturation step at 95°C for 15 min, followed by 40 cycles of 94°C denaturation for 30 s, 53.9°C annealing for 30 s and 72°C extension for 1 min, with a final extension step of 72°C for 5 min. The PCR products were visually inspected on 1.5% agarose gels to ensure amplification had occurred. Purification and sequencing of the PCR products was conducted by Macrogen (Seoul, South Korea).

Table 1. Details for each collection station, including trawling design

Latitudes and longitudes denote the start position of the middle trawl for each station. EAC, Eastern Australian Current; MOCNESS, multiple opening and closing net and environmental sensing system; NSI, North Solitary Island; RMT, rectangular mid-water trawl

Station	Latitude	Longitude	Water type	Net type	Depth	Phyllosoma standardised counts (per 10000 m^3)
1	30°01.91′S	156°52.78′E	EAC	2 Neuston nets, 2 MOCNESS	Surface, 10–100 m; 100–50 m	0
2	30°08.09′S	156°52.64′E	EAC	2 Neuston nets, 2 MOCNESS	Surface, 100–50 m; 50–10 m	0
3	27°34.15′S	153°44.05′E	Coastal	2 Neuston nets, 2 MOCNESS	Surface, 100–50 m; 50–10 m	0
4	27°41.42′S	153°46.07′E	Coastal	2 Neuston nets, 2 MOCNESS	Surface, 100–50 m; 50–10 m	0
5	28°39.10′S	154°20.33′E	Large cold core eddy	3 Neuston nets, 2 MOCNESS	Surface, 100–50 m; 50–10 m	12
6	28°46.47′S	154°20.62′E	Large cold core eddy	3 Neuston nets, 2 MOCNESS	Surface, 100–50 m; 50–10 m	0
7	28°49.90′S	154°28.80′E	Large cold core eddy	3 Neuston nets, 2 MOCNESS	Surface, 100–50 m; 50–10 m	0
8	28°57.64′S	154°31.17′E	Large cold core eddy	3 Neuston nets, 2 MOCNESS	Surface, 100–50 m; 50–10 m	4
9	32°39.563’S	153°07.48′E	Cold core frontal eddy	3 Neuston nets, 2 MOCNESS	Surface, 100–50 m; 50–10 m	4
10	32°39.92′S	153°12.81′E	Cold core frontal eddy	3 Neuston nets, 2 MOCNESS	Surface, 100–50 m; 50–10 m	0
11	32°35.21′S	153°05.23′E	Centre of cold core frontal eddy	3 Neuston nets, 2 MOCNESS	Surface, 100–50 m; 50–10 m	0
12	32°35.30′S	153°12.66′E	Centre of cold core frontal eddy	3 Neuston nets, 2 MOCNESS	Surface, 100–50 m; 50–10 m	0
13	32°32.71′S	152°40.45′E	Coastal	2 Neuston nets, 2 MOCNESS	Surface, 100–50 m; 50–10 m	0
14	32°28.68′S	152°4284’E	Coastal	2 Neuston nets, 2 MOCNESS	Surface, 100–50 m; 50–10 m	0
15	31°56.69′S	152°59.12′E	Coastal	2 Neuston nets, 2 MOCNESS	Surface, 100–50 m; 50–10 m	0
16	31°59.61′S	152°59.60′E	Coastal	0 Neuston nets, 2 MOCNESS	Surface, 100–50 m; 50–10 m	0
17	32°41.25′S	153°37.84′E	EAC	4 Neuston nets, 2 MOCNESS	Surface, 300–200 m; 100–5 m	2
18	32°42.03′S	153°35.69′E	EAC	3 Neuston nets, 2 MOCNESS	Surface, 300–200 m; 100–5 m	0
19	32°43.98′S	153°18.47′E	Centre of cold core frontal eddy	3 Neuston nets, 2 MOCNESS	Surface, 300–200 m; 100–5 m	0
20	32°44.71′S	153°19.54′E	Centre of cold core frontal eddy	3 Neuston nets, 2 MOCNESS	Surface, 400–200 m; 100–1 m	0
21	32°46.80′S	153°23.94′E	Centre of cold core frontal eddy	4 Neuston nets, 2 MOCNESS	Surface, 300–200 m; 100–5 m	2
22	32°44.75′S	153°22.23′E	Centre of cold core frontal eddy	3 Neuston nets, 2 MOCNESS	Surface, 300–200 m; 100–5 m	0
23	32°47.56′S	153°45.86′E	EAC	3 Neuston nets, 2 MOCNESS	Surface, 300–200 m; 100–5 m	0

24	32°47.68′S	153°42.20′E	EAC	3 Neuston nets, 2 MOCNESS	Surface, 300–200 m; 100–5 m	0
25	30°01.47′S	153°32.24′E	Rim of NSI Canyon	3 Neuston nets, 2 MOCNESS	Surface, 100–50 m; 50–5 m	5
26	30°01.43′S	153°33.51′E	Mid NSI Canyon	3 Neuston nets, 2 MOCNESS	Surface, 300–200 m; 100–0 m	3
27	30°02.24′S	153°36.43′E	Outer NSI Canyon	4 Neuston nets, 2 MOCNESS	Surface, 300–200 m; 100–0 m	6
28	30°01.58′S	153°32.24′E	Rim of NSI Canyon	3 Neuston nets, 2 MOCNESS	Surface, 100–50 m; 50–5 m	3
29	30°01.54′S	153°34.77′E	Mid NSI Canyon	3 Neuston nets, 2 MOCNESS	Surface, 300–200 m; 100–0 m	3
30	30°02.24′S	153°36.89′E	Outer NSI Canyon	3 Neuston nets, 2 MOCNESS	Surface, 300–200 m; 100–0 m	0
31	33°59.99′S	152°26.25′E	Warm core eddy	3 RMT nets	Surface	12
32	34°00.57′S	152°17.77′E	Warm core eddy	3 RMT nets	Surface	17
33	34°02.41′S	152°10.03′E	Warm core eddy	3 RMT nets	Surface	13
34	34°03.67′S	152°01.61′E	Warm core eddy	3 RMT nets	Surface	4

1.2.3 Data analyses

Forward and reverse sequences were manually edited and assembled in Geneious (ver. 9.0.5, Biomatters, Auckland, New Zealand). To detect the presence of potential nuclear mitochondrial DNA segments (numts), consensus *COI* sequences for each sample were translated and screened for stop codons using the invertebrate mitochondrial genetic code and all six frames in Geneious. Sequences passing numt screening were queried against the Species Level Barcode Records, which contains all barcode records, in the Barcode of Life Database (BOLD; http://www.boldsystems.org/, accessed 04 Feb 2018). If a species level match (≥98% genetic similarity) was ambiguous (e.g. the sequence matched to two species with the same genetic similarity), a search was conducted using the BOLD Public Record Database, which contains only barcode records that have been published. Samples that were only able to be matched to genus level, or with no matches, were searched against National Center for Biotechnology Information (NCBI) GenBank using BLASTn, and the top hit was recorded. If a sample obtained a hit with a percentage similarity below the threshold for a positive species identification (<98% similarity), morphological examination was undertaken using the key of the species identified in the hit (if a key was available for that species). All *COI* sequences passing numt screening were deposited in GenBank under accession numbers MK371319–MK371352.

To ensure misidentified *COI* sequences where not used as reference sequences in the species identification maximum likelihood (ML) tree, all available *COI* sequences with length ≥500 bp (where possible) were downloaded from GenBank for all Australian palinurid and scyllarid lobster species (Codes for Australian Aquatic Biota; Rees *et al*. 1999). If a *COI* sequence was not available for an Australian species, *COI* sequences from other species within the same genus were substituted. When more than 10 sequences were available for a

species, all sequences were downloaded, aligned using the Geneious MAFFT plug-in (ver. 7.309; Katoh *et al*. 2002; Katoh and Standley 2013), a neighbour joining (NJ) tree was constructed in Geneious (ver. 9.1.8) and the 10 most divergent sequences were selected for further analysis. Alignments and NJ trees were constructed for the 10 most divergent palinurid and scyllarid reference sequences. Any reference sequences that did not group with their species clade were removed from further analyses. From the sequences that did form species clades, the two most divergent sequences were chosen for each species and used as reference sequences in the species identification trees (Table 2).

To build the ML trees, *COI* sequences were aligned with MAFFT and trimmed to 545 bp to reduce sequence length disparity. The most appropriate nucleotide substitution models were calculated in jModelTest (ver. 2.1.7, http://code.google.com/p/jmodeltest2; Guindon and Gascuel 2003; Darriba *et al*. 2012) according to the corrected Akaike information criterion (AIC; Akaike 1974). The ML trees were estimated with the Geneious PhyML plug-in (ver. 2.2.3; Guindon *et al*. 2010) using the predetermined nucleotide substitution model, invariable sites and gamma distribution with 1000 bootstraps. Initially we produced a ML tree that included all our samples and the palinurid and scyllarid reference sequences to determine which family the samples belonged to. To improve the clarity of the tree, we then separated the samples into family groups and built ML trees for the palinurid and scyllarid sequences separately, using a scyllarid sequence and a palinurid sequence as the outgroup for the trees respectively. A consensus tree was determined from the 1000 bootstrapped trees. Trees built with the 10 most divergent sequences and our samples are shown in Fig. S1 and S2, available as Supplementary material to this paper.

Table 2. Lobster species and GenBank accession numbers for the cytochrome *c* oxidase I (*COI*) sequences used as reference sequences in the maximum likelihood tree

Palinuridae species	Accession number	Scyllaridae species	Accession number
Jasus edwardsii	AF192877	*Acantharctus ornatus*	JN701667
Jasus edwardsii	JF775572	*Antarctus mawsoni*	EU982702
Linuparus sordidus	JF775562	*Arctides regalis*	JN701651
Linuparus sordidus	JF775564	*Arctides regalis*	JN701652
Linuparus trigonus	JF775569	*Bathyarctus rubens*	JN701669
Linuparus trigonus	JF775571	*Biarctus vitiensis*	JN701670
Panulirus cygnus	AF339453	*Chelarctus aureau*	JF411065
Panulirus cygnus	KT696496	*Chelarctus crosnieri*	JX486086
Panulirus femoristriga	MG062676	*Chelarctus cultrifer*	JX486082
Panulirus homarus	KJ802750	*Chelarctus cultrifer*	JX486084
Panulirus homarus	KF715532	*Eduarctus martensii*	JN701671
Panulirus homarus homarus	JQ229912	*Galearctus aurora*	GU289680
Panulirus homarus homarus	KX275311	*Galearctus aurora*	JN701672
Panulirus longipes bispinosus	AB193071	*Galearctus avulsus*	JF331656
Panulirus longipes bispinosus	AB237598	*Galearctus kitanoviriosus*	JF331658
Panulirus longipes longipes	AF339464	*Galearctus rapanus*	JF331657
Panulirus longipes longipes	KF548578	*Galearctus timidus*	JN701673
Panulirus ornatus	AF339467	*Gibbularctus gibberosus*	JN701674
Panulirus ornatus	KU523815	*Ibacus alticrenatus*	JN701660
Panulirus penicillatus	AB576724	*Ibacus alticrenatus*	JN701659
Panulirus penicillatus	KF828010	*Ibacus chacei*	JN701663
Panulirus polyphagus	AF339469	*Ibacus chacei*	JN701662
Panulirus polyphagus	JN418939	*Ibacus ciliatus*	JN701661
Panulirus stimpsoni	AF339471	*Ibacus ciliatus*	JX502992
Panulirus stimpsoni	GQ292768	*Ibacus novemdentatus*	JX502993
Panulirus versicolor	KF548584	*Ibacus peronii*	JN701664
Panulirus versicolor	MG062680	*Ibacus peronii*	JN701665
Projasus parkeri	EF546343	*Parribacus antarcticus*	KJ150679
Projasus parkeri	FJ174953	*Parribacus antarcticus*	MF490044
Puerulus angulatus	JX486078	*Parribacus calendonicus*	KJ150683
Puerulus angulatus	HQ241554	*Petrarctus demani*	EU982694
Puerulus velutinus	JX629764	*Petrarctus rugosus*	EU982698
Sagmariasus verreauxi[A]	AB859775	*Petrarctus rugosus*	MF669474
Sagmariasus verreauxi	AF192883	*Remiarctus bertholdii*	JN701675
Sagmariasus verreauxi	NC_022736	*Scammarctus batei*	JF411066
		Scyllarides brasiliensis	JX896715
		Scyllarides brasiliensis	KF827966
		Scyllarides haanii	JN701655
		Scyllarides squammosus[A]	KX373661
		Scyllarides squammosus	KX373663
		Scyllarides squammosus	KX275388
		Scyllarus arctus	JQ623991
		Scyllarus arctus	KC789473
		Scyllarus chacei	JN701678
		Scyllarus chacei	KF827965
		Thenus australiensus	HM015433
		Thenus indicus	JN165725
		Thenus indicus	JQ229891
		Thenus orientalis	JN165731
		Thenus orientalis	KT224362
		Thenus parindicus	HM015425
		Thenus parindicus	HM015426

[A]Sequences used as outgroups for the palinurid and scyllarid maximum likelihood trees.

To assess the distribution and abundance of species within the EAC, phyllosoma collected in the live sort at each station were standardised to the number of phyllosoma collected per 10 000 m^3 of trawled water. The distribution and abundance of phyllosoma within the EAC was visually represented by transposing standardised catch pie charts onto a map with the R packages MAPS (ver. 3.3.0, see https://CRAN.R-project.org/package=maps), SCATTERPIE (ver. 0.0.8, see https://CRAN.R-project.org/package=scatterpie) and GGPLOT2 (ver. 2.2.1, see https://CRAN.R-project.org/package=ggplot2). For phyllosomas identified to species level, developmental stages were determined using the keys of Prasad and Tampi (1959), Tampi and George (1975), Kittaka *et al*. (1997), Matsuda and Yamakawa (2000), Matsuda *et al*. (2006), Palero *et al*. (2016) and Wakabayashi *et al*. (2017). Staging was tentatively determined for phyllosoma identified to genus level with the key of Higa *et al*. (2005).

To examine differences in the mean abundance of phyllosoma among the different water types sampled (Table 1), one-way analysis of variance (ANOVA) was performed on square root-transformed abundance data for all collected phyllosoma (i.e. palinurids, scyllarids and unidentified samples) and separately for the phyllosoma identified as palinurids and scyllarids. Assumptions of data normality and homogeneity of variance were assessed using Q–Q plots and Bartlett's test respectively. *Post hoc* Tukey's honest significant difference (HSD) tests were used to identify significant differences in the mean abundance of phyllosoma among water types. The homogeneity of variances assumption could not be satisfied for the raw or transformed palinurid data. Consequently, two-sample *t*-tests, assuming unequal variances, were used to compare the mean abundance palinurid phyllosoma between: (1) the warm core eddy and canyon; and (2) the warm core eddy and the cold core frontal eddy. These three water types were the only features in which palinurids

were identified. The critical *P*-value of 0.05 was maintained across the two simultaneous *t*-tests using the conservative Bonferroni correction (critical $P = 0.05/2 = 0.025$ for each of the two tests). Statistical tests were performed using the 'aov', 'anova', 'TukeyHSD' and 't.test' commands in R.

Distribution maps were produced for species identified by DNA barcoding in the phyllosoma samples. These maps contained the species distribution obtained from International Union for Conservation of Nature (IUCN) Red List shapefiles (https://www.iucnredlist.org/resources/spatial-data-download, accessed 22 Mar 2016), as well as the corresponding phyllosoma collection sites, and were created using the R packages MAPS, MAPTOOLS (ver. 0.9-2, see https://cran.r-project.org/package=maptools), MAPDATA (ver. 2.2.6, see https://cran.r-project.org/package=mapdata), GGMAP (ver 2.6.1, see https://cran.r-project.org/package=ggmap) and GGPLOT2. The minimum dispersal distance of the phyllosoma collected outside their known adult range was measured by loading the species distribution shapefiles and collection sites into Google Earth Pro (ver. 7.3.1.4507, Google Inc., Mount View, CA), where the distance between the nearest species distribution and the phyllosoma collection points were measured and averaged.

1.3 Results

1.3.1 Species identifications with COI

In total, 56 phyllosoma and 1 nisto (post-larval stage for slipper lobsters) were collected for molecular analysis, with high-quality sequences obtained from 53 of the samples. From the high-quality samples, 35% of sequences ($n = 19$) contained stop codons, indicating the sequences originated from the nuclear genome, and consequently these sequences were removed from all further analyses. Of the 34 remaining sequences, 12 definite species

matches (>98% genetic similarity; Table 3) were made through the BOLD Species Level Database with an additional three species matches obtained through the BOLD Public Record Database (>98% genetic similarity; Table 3). The ML tree reflected the BOLD species matches because sequences from the phyllosoma samples formed clades with the same species identified in BOLD (Fig. 1).

Five phyllosoma samples were identified to the genus *Scyllarides* using BOLD but could not be identified to species level within this genus. This was due to a single *Scyllarides brasiliensis* (Accession no. JN701654) sequence exhibiting the same genetic similarity (99.4%) as *Scyllarides squammosus* to the sample sequence, whereas all other *S. brasiliensis* sequences had a genetic similarity below 92.8%. The NJ tree created to check the quality of the reference sequences showed that all *S. brasiliensis* sequences formed a monophyletic group, except for JN701654, which created a clade with *S. squammosus* (see Fig. S3). This suggests the *S. brasiliensis COI* sequence has been misidentified and is likely to be *S. squammosus*. The top BLAST hit in NCBI identified the five phyllosoma samples to *S. squammosus*, which was further supported by the five samples forming a monophyletic group with *S. squammosus* in the ML tree (Fig. 1).

Two samples (R34_03_5 and R35_03_1) indicated high genetic similarity to both *Panulirus longipes bispinosus* and *Panulirus longipes femoristriga* (Table 3) in the GenBank analyses. The *P. l. bispinosus* (Accession no. AB193071) and *P. l. femoristriga* (Accession no. AF339463) sequences had high sequence similarity, differing by only 1 bp, which was located towards the end of the sequence. It is likely that the sequence AB193071 has been misidentified and is actually *P. l. bispinosus*; therefore, the *P. l. femoristriga* sequence was not used as a reference in the ML tree. The ML tree indicated that the species identified as *P.*

longipes in BOLD were more closely related to the subspecies *P. l. bispinosus* than to *P. l. longipes*.

Eleven of the phyllosoma sequences could not be matched to any species or genera within the BOLD database (Table 3). Of these, eight samples likely represented a single species because they formed part of a short-branched clade within the genus *Galearctus* (Fig. 1*b*), although no reference sequence exhibited a genetic similarity high enough (>98%) for a positive identification. Sample N26_02 matched at 96% similarity with *Galearctus timdus*, which is below the genetic similarity threshold for a positive species identification. An identification key was only available for *Galearctus kitanoviriosus*; therefore, morphological analysis was unable to provide a species match for the samples within the *Galearctus* spp. clades. Sample R32_03_6 fell within the *Panulirus* clade, but did not form a monophyletic group with any of the reference sequences and exhibited only 96% similarity to *P. l. bispinosus*. Sample EZ05_01_2 formed a well-supported relationship with *Eduarctus martensii*, albeit with long branch lengths and a sequence similarity of 84.4%. Although the species and genus of EZ05_01_2 remains unresolved with *COI* barcoding, morphological examination indicates the distal ends of the uropods are pointed and the telson has lateral spikes, both of which are defining features of *E. martensii* phyllosoma (Phillips and McWilliam 1986b).

Overall, from the 34 identifiable sequences in Table 3, 19 samples belong to the Family Palinuridae and 15 belong to the Family Scyllaridae. Within the palinurid samples, 13 were identified as *P. l. bispinosus*, 3 as *P. versicolor*, 1 as *P. penicillatus*, 1 as *S. verreauxi* and 1 was unidentified. Within the scyllarid samples, five were identified as *Scyllarides squammosus* and nine were identified as *Galearctus* spp., with eight samples belonging to one species and one sample to another species. One sample was only identifiable to the

Family Scyllaridae through DNA barcoding; however, morphological examination indicated this sample was *E. martensii*.

Table 3. Top species matches and genetic similarity for phyllosoma collected on the 2015 *RV Investigator* voyage

The first number in the Sample ID indicates the station where the phyllosoma was collected. Superscript lowercase letters signify the databases used for species identifications, as follows: a, Barcode of Life Database (BOLD) Species Level Barcode Records; b, BOLD, Public Record Barcode Database; c, only genus match available in BOLD, top GenBank species match is reported; d, no sequence matches were available in BOLD, top GenBank species match is reported

Sample ID	Top species match	Genetic similarity (%)	Stage
N05_01	*Galearctus rapanus*[d]	90.0	–[A]
EZ05_01_2	*Eduarctus martensii*[d]	84.4	IX
N08_03	*Galearctus rapanus*[d]	91.0	IX
EZ08_05	*Galearctus rapanus*[d]	91.0	IX
N09_03	*Panulirus versicolor*[b]	99.6	XI[B]
N17_02	*Scyllarides squammosus*[c]	99.4	IX
N21_01	*Scyllarides squammosus*[c]	99.8	IX
N25_01_1	*Galearctus rapanus*[d]	91.0	V
N26_02	*Galearctus timidus*[d]	96.0	IX
N27_01	*Scyllarides squammosus*[c]	99.4	X
EZ28_03	*Galearctus rapanus*[d]	91.0	Nisto
Stn29_Flo	*Panulirus versicolor*[b]	99.6	XI[B]
R32_02_1	*Panulirus longipes*[a]	99.3	IX
R32_02_2	*Panulirus longipes*[a]	99.4	VII
R32_02_3	*Scyllarides squammosus*[c]	99.8	IX
R32_03_3	*Galearctus rapanus*[d]	90.0	VIII
R32_03_4	*Panulirus longipes*[a]	99.2	–[A]
R32_03_6	*Panulirus longipes bispinosus*[d]	96.0	VII
R33_01_4	*Panulirus longipes*[a]	99.3	VII
R33_02_5	*Panulirus longipes*[a]	99.8	VIII
R33_02_8	*Panulirus versicolor*[a]	99.3	IX
R33_03_1	*Scyllarides squammosus*[c]	99.8	VIII
R33_03_3	*Panulirus longipes*[a]	99.8	VII
R34_01_1	*Panulirus longipes*[a]	99.4	VIII
R34_02_1	*Sagmariasus verreauxi*[a]	99.8	XIII
R34_02_2	*Panulirus longipes*[a]	99.3	VIII
R34_03_2	*Galearctus rapanus*[d]	91.0	VIII
R34_03_3	*Panulirus longipes*[a]	99.1	VII
R34_03_4	*Galearctus rapanus*[d]	91.0	VIII
R34_03_5	*Panulirus longipes bispinosus*[d]	98.3	VII
	Panulirus longipes femoristriga[d]	98.2	
R35_01_1	*Panulirus longipes*[a]	100.0	IX
R35_01_2	*Panulirus longipes*[a]	99.8	IX
R35_01_3	*Panulirus penicillatus*[a]	99.8	VIII
R35_03_1	*Panulirus longipes bispinosus*[d]	98.3	VIII
	Panulirus longipes femoristriga[d]	98.3	

[A]Specimen unable to be staged because it was badly damaged.

[B]Key for staging only available to Stage XI.

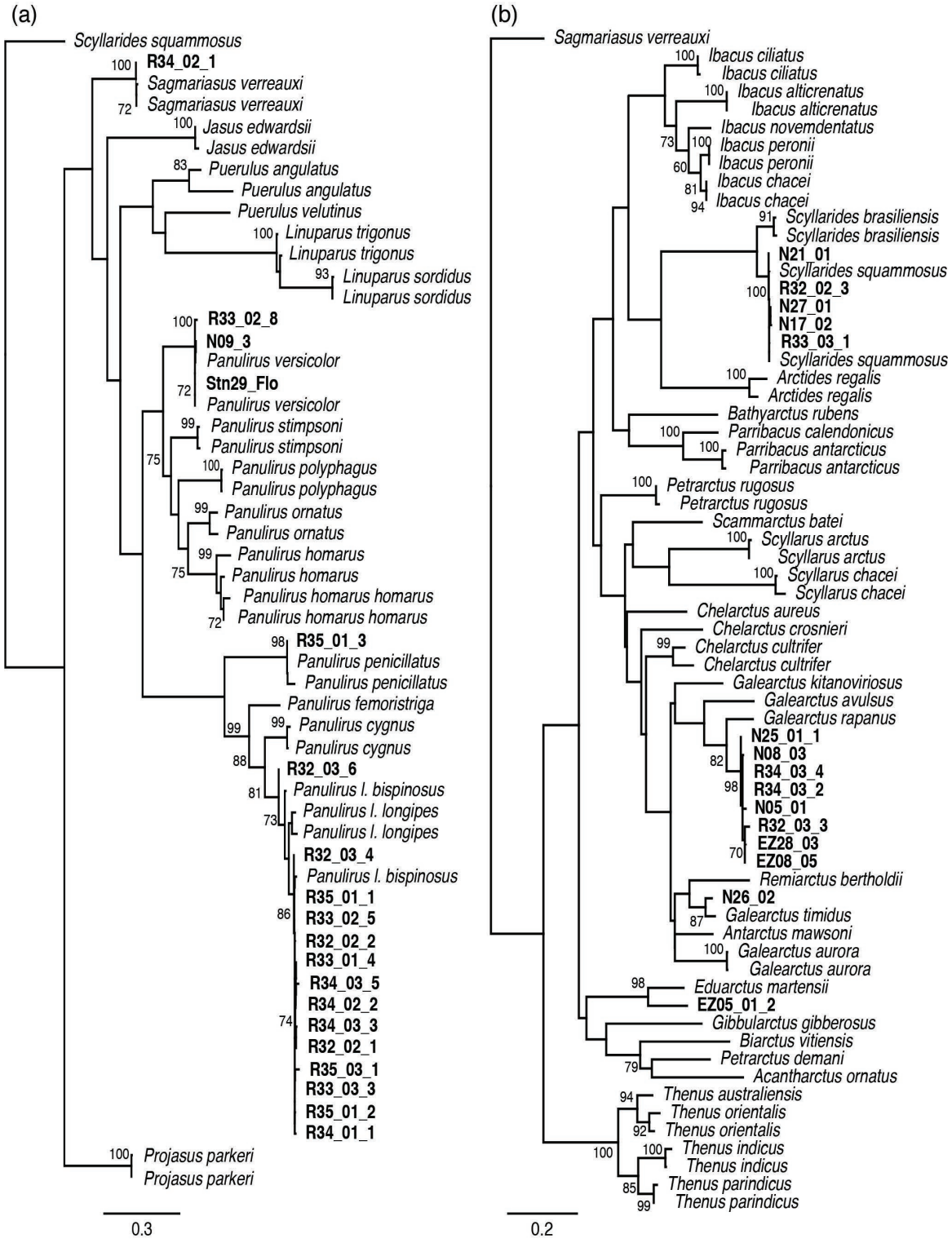

Fig. 1. Molecular species identification of phyllosoma collected along the east Australian coast using maximum likelihood trees for (a) palinurid and (b) scyllarid species. The trees are based on cytochrome c oxidase I sequences, with substitution models and outgroups of (a) Hasegawa, Kishino and Yano model and *Scyllarides squammosus* and (b) Generalised Time

Reversible model and *Sagmariasus verreauxi*. Collected samples are denoted in bold by letter–number combinations. All reference sequences were downloaded from GenBank. Node labels represent bootstrap values from 1000 replicates.

1.3.2 Phyllosoma species assemblage and spatial distribution

Phyllosoma distribution (palinurids, scyllarids and unidentified samples combined) was heterogeneous across the multiple water types sampled. Standardised abundances (phyllosoma per 10 000 m^3 of seawater) highlight that the highest catches of live sorted phyllosoma occurred at Stations 5, 32, 33 and 34 (Fig. 2), which were situated within large cold or warm core eddies. Comparisons of the distribution of all phyllosoma collected indicated a significantly higher abundance of phyllosoma within the warm core eddy than in the EAC or cold core frontal eddy ($F_{4,23} = 8.07$, $P = 0.0003$). Phyllosoma were absent from live sorted catches at 59% of stations, and at all the stations situated in coastal water (Table 1). When examined separately, scyllarid phyllosoma abundance was homogeneous across water types ($F_{4,23} = 2.30$, $P = 0.0897$), whereas palinurid phyllosoma exhibited significantly higher abundance in the warm core eddy than in the cold core frontal eddy ($t_{3.073} = 4.526$, $P = 0.019 < 0.025$) and in the canyon ($t_{3.185} = 4.421$, $P = 0.019 < 0.025$). Although scyllarid phyllosoma were equally abundant across all water types, it was apparent that net hauls containing phyllosoma at the northern stations (1–30) primarily consisted of scyllarid phyllosoma, whereas net hauls at the southern stations (31–34) had higher numbers of palinurid phyllosoma.

Phyllosoma from three species, namely *P. l. bispinosus*, *P. versicolor* and *P. penicillatus*, were collected outside their known adult species distributions (Fig. 3). *P. l. bispinosus*

phyllosoma were collected on average ~75 km south of Woolnough Knoll, off the coast of Sydney, Australia, their nearest known adult distribution (Fig. 3*a*). The phyllosoma of *P. versicolor* were collected on average ~1300 km south-west of South Bellonia Reef, New Caledonia, their nearest known distribution (Fig. 3*c*). *P. penicillatus* was collected ~1800 km south-west of New Caledonia, their nearest known adult distribution (Fig. 3*b*). All *P. l. bispinosus*, *P. versicolor*, *P. penicillatus* and *S. squammosus* samples were identified as late-stage phyllosoma (Table 2).

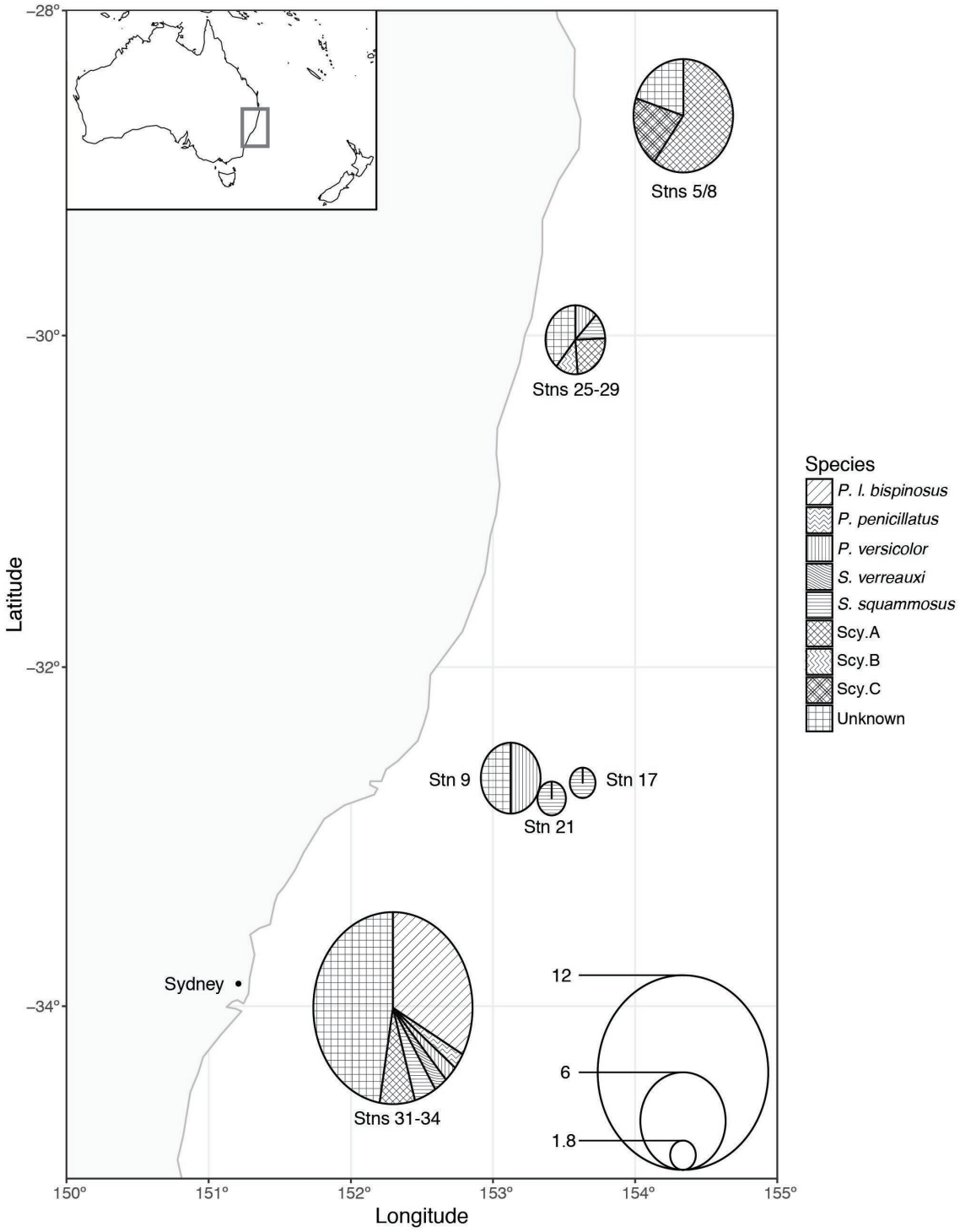

Fig. 2. Locations at which phyllosoma were collected along the eastern Australian coast in June 2015 for *Panulirus longipes bispinosus*, *Panulirus penicillatus*, *Panulirus versicolor*, *Sagmariasus verreauxi*, *Scyllarides squammosus*, unknown Scyllaridae species (Scy.A, Scy.B, Scy.C) and unknown lobster species. Pie charts denote the species collected (pattern fills) and are scaled with standardised abundance (number of phyllosoma per 10 000 m3).

Counts from Stations (Stn) 5 and 8, Stn 25–29 and Stn 31–34 were combined for clarity, as they represent the same water type. Morphological examination indicates Scy.C is potentially *Eduarctus martensii*.

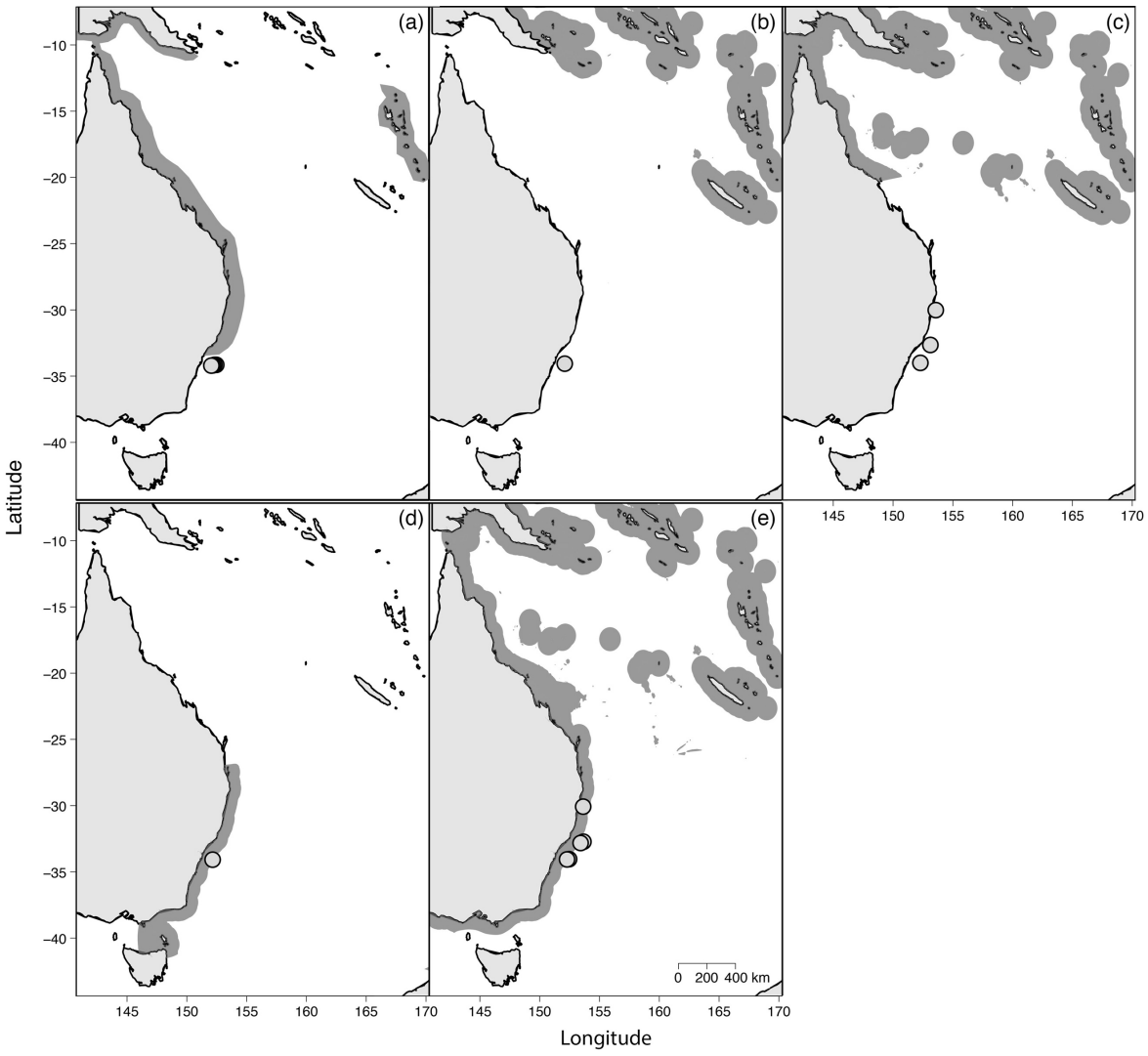

Fig. 3. Species distribution maps for (a) *Panulirus longipes bispinosus*, (b) *Panulirus penicillatus*, (c) *Panulirus versicolor*, (d) *Sagmariasus verreauxi* and (e) *Scyllarides squammosus*. Maps are centred on the eastern coast of Australia. The known distribution of the species is indicated in dark grey. Sites of phyllosoma collection are denoted by circles.

1.4 Discussion

In this study we investigated the species assemblage and spatial distribution of phyllosoma samples, collected within a WBC along the mid-eastern Australian coast. To do this we first assessed the utility of the *COI* gene as a barcoding region for species-level identification of phyllosoma. We found that potential numts were amplified in 35% of phyllosoma samples, indicating the *COI* barcoding region is suboptimal for the identification of phyllosoma samples to species level. We then examined the spatial distribution of phyllosoma and found the highest phyllosoma abundances were associated with large eddies. Scyllarid phyllosoma exhibited relatively homogeneous abundances across water types, whereas palinurid phyllosoma abundances were heterogeneous and with highest numbers collected within a warm core eddy, which was the most southern oceanographic feature sampled. Phyllosoma of three species, namely *P. l. bispinosus*, *P. versicolor* and *P. penicillatus*, were collected on average between 75 and 1800 km south of their known adult distributions, exhibiting the high dispersal capabilities of these individuals.

1.4.1 Performance of COI barcoding region for identifying phyllosoma

Due to the high prevalence of potential numts identified within our phyllosoma samples, we suggest that using only the *COI* gene for species identification of phyllosoma samples is suboptimal. Species barcoding is based on the assumption that all genetic regions used are orthologous (i.e. genes present in different species have evolved from a common ancestor); however, numts are paralogues (i.e. genes that arose from duplication within a genome resulting in the presence of multiple gene copies) and, if unwittingly used, results in incorrect inferences (Song *et al*. 2008; Buhay 2009). There is evidence that the presence of numts is correlated with the size of the genome (Bensasson *et al*. 2001) and because lobsters have large genomes (e.g. Palinuridae c-values: 5.55–3.15; Scyllaridae c-values: 6.82–1.94; Deiana

et al. 1999; Jimenez *et al*. 2010) it is not surprising that we detected a high prevalence of numts within our samples. It is important for studies to report the presence of numts, when found, to gain a better understanding of the most appropriate barcodes to use for different taxa. A universal barcode may not be feasible for some taxa such as palinurids and scyllarids.

Although steps can be taken to reduce the likelihood of sequencing numts (e.g. using mitochondria-rich tissues, reverse transcription PCR or long PCR; Bensasson *et al*. 2001), these methods are not always effective (Song *et al*. 2008). Although examining the utility of the *16S* region as a DNA barcode was outside the scope of the present study, this region should be examined empirically to determine its reliability as a species identification tool for palinurid and scyllarid lobsters. If the *16S* region was also found to have a high prevalence of numts, other potential barcoding candidates are the *12S* rRNA mitochondrial region, which has been used within palinurid and scyllarid lobsters for phylogenetic analyses (Bracken-Grissom *et al*. 2014).

For the 65% of sequences not identified as numts, 28% of the phyllosoma sequences were unable to be identified to species level with either the BOLD or GenBank databases. Sample EZ05_01_2 exhibited morphological characteristics of *E. martensii*, but was unable to be positively identified from the publicly available *E. martensii COI* sequence. *COI* amplification has been reported to be difficult with *E. martensii*, and *16S* may be a more appropriate barcode for this species (Wakabayashi *et al*. 2017). The remaining unidentified sequences likely represent two different scyllarid species because they form close relationships with two *Galearctus* spp. clades, indicating the existence of species barcoding data gaps within the Family Scyllaridae. Of the 33 scyllarid species reported to occur within Australian waters (Rees *et al*. 1999), 12 species from 6 genera lack *COI* reference sequences.

For five of these genera, *COI* sequences are available for non-Australian species and can be used to represent the genus, with only the *Crenarctus* genus lacking *COI* representation entirely. One clade of the unidentified *Galearctus* spp. is likely to be *Galearctus umbilicatus* because it is the only known *Galearctus* sp. that occurs within Australian waters, along the NSW and Queensland coasts (McWilliam *et al*. 1995; Holthuis 2002), and lacks *COI* representation on publicly available databases. The potential identity of the second *Galearctus* clade is unclear. The only other known unrepresented *Galearctus* spp. is *Galearctus lipkei* (Yang and Chan 2010), although this species is only known to occur in Taiwanese waters.

A factor hindering the identification of species with barcodes is the publication of misidentified barcodes (Carew *et al*. 2017). For example, in this study we discovered two misidentified *COI* sequences that had been published and were publicly available in the BOLD or GenBank database(s). The BOLD database included a sequence that had been referenced as *S. brasiliensis* but was clearly a *S. squammosus COI* sequence, which meant we were unable to use BOLD to gain a reliable species identification and were required to investigate further. In GenBank we discovered a naming inconsistency with a *P. l. femoristriga COI* barcode. The subspecies *P. l. femoristriga* was reclassified as *Panulirus femoristriga*, a separate species (Chan and Ng 2001; Ravago and Juinio-Menez 2002). Thus the *P. l. femoristriga* barcode should be *P. femoristriga* under the new classification; however the *P. l. femoristriga* barcode differed by only 1 bp from *P. l. bispinosus*, and hence appears to have been misclassified. The publication in which this sequence is originally reported reflects this naming change (Ptacek *et al*. 2001), but the barcode in GenBank does not. Without prior knowledge of the species reclassification, further investigations are unnecessarily required. Species identifications through barcoding can only be as good as the

reference barcodes, and thus more stringent processes are needed to ensure the published barcode sequences are correctly identified before uploading the sequences onto public databases (discussed in Collins and Cruickshank 2013; Carew *et al*. 2017).

Due to the reclassification of *P. l. femoristriga* with *P. l. bispinosus*, we will refer to the samples that were identified as both subspecies as *P. l. bispinosus* from here on in. Other plankton trawl studies conducted on the eastern coast of Australia have reported phyllosoma collections of *P. l. femoristriga* (McWilliam and Phillips 1983; Dennis *et al*. 2001). However, these studies were conducted before the species were reclassified, therefore it is possible that the phyllosoma in these studies were *P. l. bispinosus*. It should be noted that they may also be *P. femoristriga*, which is difficult to differentiate from *P. longipes* subspecies through morphology alone (Ravago and Juinio-Menez 2002; Chow *et al*. 2006*a*). It should also be noted that since the revision of the *P. longipes* species complex there is some uncertainty in the distributions of *P. l. longipes*, *P. l. bispinosus* and *P. femoristriga* (Chan *et al*. 2011).

1.4.2 Phyllosoma spatial distribution within the EAC

This study represents a snapshot in time, providing insight into the mid-year spatial distribution of phyllosoma within the EAC, a WBC. Our results indicate a disparity in distributions of scyllarid and palinurid phyllosoma, with scyllarids presented across water types, whereas palinurids were concentrated in a warm water eddy at the lower latitude sampling stations. Due to this distribution disparity, different larval species assemblages were evident at higher-latitude stations compared with lower-latitude stations, with scyllarid species more dominant at the northern sites, situated within a cold core eddy, and palinurid species more dominant at the southern sites, situated in a warm water eddy. The distribution disparity may be reflective of the shorter pelagic larval duration of scyllarid phyllosoma compared with palinurids (Lavalli and Spanier 2007), which may result in scyllarid

phyllosoma staying closer to their adult distribution. This was reflected in our results; the scyllarid species that were identified all had adult distributions within the sampled areas. The majority of the palinurid species collected within the warm core eddy were tropical species, supporting a previously proposed hypothesis that warm core EAC eddies are important for the transport of tropical biota to higher latitudes (Smith and Simpson 1991). All staged individuals were of similar developmental stages regardless of the water type they were associated with, indicating they were possibly entrained into the EAC and its associated eddies from the same cohort.

Phyllosoma densities were the highest in eddies, whereas considerably fewer phyllosoma were collected within the southward-flowing EAC waters and none were collected within coastal water. The absence of phyllosoma in these waters is most likely due to the high rates of flow in these waters and the time elapsed between spawning and the survey. Consequently, there is great potential for advection of phyllosoma away from coastal spawning sites. The results of this study are in contrast with those reported by McWilliam and Phillips (1983), where phyllosoma were common in both a warm core EAC eddy and the surrounding EAC waters. Cold and warm core eddies are known to entrain and retain phyllosoma in Western Australia and New Zealand (Chiswell and Booth 1999; Säwström *et al*. 2014; Wang *et al*. 2015) and EAC eddies are thought to act as planktonic incubators (Suthers *et al*. 2011), which is a model supported by the results of the present study. However, because the eddies in this paper are inextricably linked with latitude, additional phyllosoma surveys should be conducted to further investigate the association of phyllosomas with eddies in the EAC.

The occurrence of phyllosoma from three tropical palinurid lobster species, collected ~75–1800 km to the south or south-west of their known adult distributions, reflects the high

dispersive capabilities of the larvae of these lobsters. The phyllosoma of the tropical species *P. penicillatus* and subtropical *P. l. bispinosus* were all classed as late-stage phyllosoma, nearing the end of their larval duration of 7–11 months (*P. penicillatus*; Johnson 1971; Matsuda *et al*. 2006) and 9–10 months (*P. l. bispinosus*; Matsuda and Yamakawa 2000). Our results corroborate those of McWilliam and Phillips (1983), who discovered late-stage *P. l. femoristriga*, *P. penicillatus* and *P. versicolor* phyllosoma as far south as the Bass Strait (the water mass between mainland Australia and Tasmania). The dispersal limit for *P. penicillatus* and *P. versicolor* phyllosoma that are able to return to adult populations is thought to be contained within the Coral Sea Gyre bounded by the continental shelves of north Queensland and Papua New Guinea (Dennis *et al*. 2001). Occurrence of phyllosoma of these species within temperate waters is interpreted as larval attrition (McWilliam and Phillips 1983; Dennis *et al*. 2001) because it is unlikely lecithotrophic puerulus (spiny lobster postlarvae with directional swimming capabilities) have the capacity to swim countercurrent for >1000 km to return to their adult range within the puerulus time frame, which is 16–19 days for *P. penicillatus* (Jeffs *et al*. 2005; Matsuda *et al*. 2006). The present study and the study of McWilliam and Phillips (1983) illustrate that larvae of tropical lobster species have the dispersal capabilities to expand their range poleward if environmental conditions become favourable in the future to enable settlement and establishment.

In summary, although DNA barcoding is a useful resource, the high prevalence of potential numts sequenced from the *COI* region in palinurid and scyllarid lobsters suggests other barcoding regions should be considered for species identification within these taxa. This study highlights the importance of carefully examining publicly available *COI* sequences for naming inconsistencies before including sequences as references in species identification studies. Although adult *P. l. bispinosus*, *P. versicolor* and *P. penicillatus* are not currently

distributed in the south of NSW, phyllosoma of these tropical palinurid lobsters are being transported poleward to this area by warm water EAC eddies. As waters warm in this area, these three species may have the opportunity to undergo settlement, the first step of a range shift. Further plankton studies should track the spatial distribution and abundance of tropical phyllosoma within EAC waters and determine the thermal tolerance of these species at different life stages. With this information, simulations predicting the future distribution of tropical palinurid species could be conducted and species with the potential to become established could be monitored, providing an early range shift detection warning to resource managers whose fisheries may be affected.

Acknowledgements

We would like to thank all of Marine National Facilities Staff and scientific crew aboard the *RV Investigator*. We would especially like to thank Tony Miskiewicz, Valquiria Garcia, Derrick Cruz, Steven Hawkin, Hayden Schilling, Vivian Yeung and Elisa Holgate who were all members of the plankton live sorting crew that assisted in the phyllosoma collections. This research was funded by ARC DP 150101491 and a La Trobe University Securing Food, Water and Environment Grant. Support for AJ came from an Australian Research Council Linkage Project No. LP150100064, and an OECD Co-operative Research Programme Fellowship. This research is a contribution to the Worldwide Universities Network project; Ocean Eddies in a Changing Climate: Understanding the Impact of Coastal Climates and Fisheries Production.

Conflicts of Interest

The authors declare no conflicts of interest.

References

Akaike, H. (1974). A new look at the statistical model identification. *IEEE Transactions on Automatic Control* **19**, 716–723.

Bensasson, D., Zhang, D., Hartl, D.L. and Hewitt, G.M. (2001). Mitochondrial pseudogenes: evolution's misplaced witnesses. *Trends in Ecology & Evolution* **16**, 314–321.

Bates, A.E., Pecl, G.T., Frusher, S., Hobday, A.J., Wernberg, T., Smale, D.A., Sunday, J.M., Hill, N.A., Dulvy, N.K., Colwell, R.K., Holbrook, N.J., Fulton, E.A., Slawinski, D., Feng, M., Edgar, G.J., Radford, B.T., Thompson, P.A. and Watson, R.A. (2014). Defining and observing stages of climate-mediated range shifts in marine systems. *Global Environmental Change* **26**, 27-38.

Booth, D.J., Figueira, W.F., Gregson, M.A., Brown, L. and Beretta, G. (2007). Occurrence of tropical fishes in temperate southeastern Australia: role of the East Australian Current. *Estuarine, Coastal and Shelf Science* **72**, 102–114.

Booth, J. and Phillips, B. (1994). Early life history of spiny lobster. *Crustaceana* **66**, 271–294.

Booth, J.D., Webber, W.R., Sekiguchi, H. and Coutures, E. (2005). Diverse larval recruitment strategies within the Scyllaridae. *New Zealand Journal of Marine and Freshwater Research* **39**, 581–592.

Bracken-Grissom, H.D., Ahyong, S.T., Wilkinson, R.D., Feldmann, R.M., Schweitzer, C.E., Breinholt, J.W., Bendall, M., Palero, F., Chan, T., Felder, D.L., Robles, R., Chu, K., Tsang, L., Kim, D., Martin, J.L. and Crandall, K.A. (2014). The emergence of lobsters: phylogenetic relationships, morphological evolution and divergence time comparisons of an ancient group (Decapoda: Achelata, Astacidea, Glypheida, Polychelida). *Systematic Biology* **63**, 457–479.

Brandt, S. (1981). Effects of a warm-core eddy on fish distributions in the Tasman Sea off

East Australia. *Marine Ecology Progress Series* **6**, 19–33.

Buhay, J.E. (2009). 'COI-like' sequences are becoming problematic in molecular systematic and DNA barcoding studies. *Journal of Crustacean Biology* **29**, 96–110.

Canto-García, A.A., Goldstein, J.S., Sosa-Cordero, E. and Carrillo, L. (2016). Distribution and abundance of *Panulirus* spp. phyllosomas off the Mexican Caribbean coast. *Bulletin of Marine Science* **92**, 207–227.

Carew, M.E., Nichols, S.J., Batovska, J., St Clair, R., Murphy, N.P., Blacket, M.J. and Shackleton, M.E. (2017). A DNA barcode database of Australia's freshwater macroinvertebrate fauna. *Marine and Freshwater Research* **68**, 1788–1802.

Chan, T., Butler, M., Cockcroft, A., MacDiarmid, A. and Wahle, R. (2011). *Panulirus femoristriga* [Online]. Available at: http://dx.doi.org/10.2305/IUCN.UK.2011-1.RLTS.T170031A6714256.en.

Chan, T.Y. and Ng, P.K.L. (2001). On the nomenclature of the commercially important spiny lobsters *Panulirus longipes femoristriga* (Von Martens, 1872), *P. bispinosus* Borradaile, 1899, and *P. albiflagellum* Chan & Chu, 1996 (Decapoda, Palinuridae). *Crustaceana* **74**, 123–127.

Chiswell, S.M. and Booth, J.D. (1999). Rock lobster *Jasus edwardsii* larval retention by the Wairarapa Eddy off New Zealand. *Marine Ecology Progress Series* **183**, 227–240.

Chow, S., Suzuki, N., Imai, H. and Yoshimura, T. (2006a). Molecular species identification of spiny lobster phyllosoma larvae of the genus *Panulirus* from the northwestern Pacific. *Marine Biotechnology* **8**, 260–267.

Chow, S., Yamada, H. and Suzuki, N. (2006b). Identification of mid- to final stage phyllosoma larvae of the genus *Panulirus* White, 1847 collected in the Ryukyu Archipelago. *Crustaceana* **79**, 745–764.

Collins, R.A. and Cruickshank, R.H. (2013). The seven deadly sins of DNA barcoding.

Molecular Ecology Resources **13**, 969–975.

Cowen, R.K. and Sponaugle, S. (2009). Larval dispersal and marine population connectivity. *Annual Review of Marine Science* **1**, 443–66.

Darriba, D., Taboada, G., Doallo, R. and Posada, D. (2012). jModelTest 2: more models, new heuristics and parallel computing. *Nature Methods* **9**, 772.

Deiana, A.M., Cau, A., Coluccia, E., Cannas, R., Milia, A., Salvadori, S. and Libertini, A. (1999). Genome size and AT-DNA content in thirteen species of Decapoda. In: Schram, F. and von Vaupel Klein, J. (eds.) *Crustaceans and the Biodiversity Crisis*. Leiden, The Netherlands: Kninklijke Brill NV, pp. 981–985.

Dennis, D.M., Pitcher, C.R. and Skewes, T.D. (2001). Distribution and transport pathways of *Panulirus ornatus* (Fabricius, 1776) and *Panulirus* spp. larvae in the Coral Sea, Australia. *Marine and Freshwater Research* **52**, 1175–1185.

Flood, M., Stobutzki, I., Andrews, J., Ashby, C., Begg, G.A., Fletcher, R., Gardner, C., Georgeson, L., Hansen, S., Hartmann, K. and Hone, P. (2014). *Status of Key Australian Fish Stocks Report 2014*. Canberra.

Folmer, O., Black, M., Hoeh, W., Lutz, R. and Vrijenhoek, R. (1994). DNA primers for amplification of mitochondrial cytochrome *c* oxidase subunit I from diverse metazoan invertebrates. *Molecular Marine Biology and Biotechnology* **3**, 294–299.

García-Rodríguez, F.J., Ponce-Díaz, G., Muñoz-García, I., González-Armas, R. and Perez-Enriquez, R. (2008). Mitochondrial DNA markers to identify commercial spiny lobster species (*Panulirus* spp.) from the Pacific coast of Mexico: an application on phyllosoma larvae. *Fishery Bulletin* **106**, 204–212.

Genis-Armero, R., Guerao, G., Abelló, P., González-Gordillo, J.I., Cuesta, J.A., Corbari, L., Clark, P.F., Capaccioni-Azzati, R. and Palero, F. (2017). Possible amphi-atlantic dispersal of scyllarus lobsters (crustacea: Scyllaridae): Molecular and larval evidence.

Zootaxa **4306**, 325–338.

Guindon, S., Dufayard, J.F., Lefort, V., Anisimova, M., Hordijk, W. and Gascuel, O. (2010). New algorithms and methods to estimate maximum-likelihood phylogenies: Assessing the performance of PhyML 3.0. *Systematic Biology* **59**, 307–321.

Guindon, S. and Gascuel, O. (2003). A simple, fast and accurate method to estimate large phylogenies by maximum-likelihood. *Systematic Biology* **52**, 696–704.

Higa, T., Fujita, Y. and Shokita, S. (2005) Complete larval development of a scyllarine lobster *Galearctus kitanoviriosus* (Harada, 1962) (Decapoda: Scyllaridae: Scyllarinae), reared under laboratory conditions. *Crustacean Research* **34**, 1-26.

Holthuis, L.B. (2002). The Indo-Pacific scyllarine lobsters (Crustacea, Decapoda, Scyllaridae). *Zoosystema* **24**, 499-529.

Jeffs, A.G., Montgomery, J.C. and Tindle, C.T. (2005). How do spiny lobster post-larvae find the coast? *New Zealand Journal of Marine and Freshwater Research* **39**, 605-617.

Jimenez, A., Kinsey, S., Dillaman, R. and Kapraun, D. (2010). Nuclear DNA content variation associated with muscle fiber hypertrophic growth in decapod crustaceans. *Genome* **53**, 161–171.

Johnson, C.R., Banks, S.C., Barrett, N.S., Cazassus, F., Dunstan, P.K., Edgar, G.J., Frusher, S.D., Gardner, C., Haddon, M., Helidoniotis, F., Hill, K.L., Holbrook, N.J., Hosie, G.W., Last, P.R., Ling, S.D., Melbourne-Thomas, J., Miller, K., Pecl, G.T., Richardson, A.J., Ridgway, K.R., Rintoul, S.R., Ritz, D.A., Ross, D.J, Sanderson, J.C., Sheperd, S.A., Slotwinski, A., Swadling, K.M. and Taw, N. (2011). Climate change cascades: Shifts in oceanography, species' ranges and subtidal marine community dynamics in eastern Tasmania. *Journal of Experimental Marine Biology and Ecology* **400**, 17–32.

Johnson, M. (1971). The palinurid and scyllarid lobster larvae of the tropical eastern Pacific

and their distribution as related to the prevailing hydrography. *Bulletin of the Scripps Institution of Oceanography* **19**, 1–36.

Katoh, K., Misawa, K., Kuma, K. and Miyata, T. (2002). MAFFT: a novel method for rapid multiple sequence alignment based on fast Fourier transform. *Nucleic Acids Research* **30**, 3059–3066.

Katoh, K. and Standley, D.M. (2013). MAFFT multiple sequence alignment software version 7: Improvements in performance and usability. *Molecular Biology and Evolution* **30**, 772–780.

Keane, J.P. and Neira, F.J. (2008). Larval fish assemblages along the south-eastern Australian shelf: Linking mesoscale non-depth-discriminate structure and water masses. *Fisheries Oceanography* **17**, 263–280.

Kittaka, J., Ono, K. and Booth, D.J. (1997) Complete development of the green rock lobster, *Jasus verreauxi* from egg to juvenile. *Bulletin of Marine Science* **61**, 57-71.

Konishi, K., Suzuki, N. and Chow, S. (2006). A late-stage phyllosoma larva of the spiny lobster *Panulirus echinatus* Smith, 1869 (Crustacea: Palinuridae) identified by DNA analysis. *Journal of Plankton Research* **28**, 841–845.

Lavalli, K. L., & Spanier, E. (Eds.). (2007). The biology and fisheries of the slipper lobster. CRC press, Boca Raton, FL, USA.

Ling, S.D., Johnson, C.R., Ridgway, K., Hobday, A.J. and Haddon, M. (2009). Climate-driven range extension of a sea urchin: inferring future trends by analysis of recent population dynamics. *Global Change Biology* **15**, 719–731.

Lobel, P.S. and Robinson, A.R. (1988). Larval fishes and zooplankton in a cyclonic eddy in Hawaiian waters. *Journal of Plankton Research* **10**, 1209–1223.

Matear, R.J., Chamberlain, M.A., Sun, C. and Feng, M. (2013). Climate change projection of the Tasman Sea from an eddy-resolving ocean model. *Journal of Geophysical*

Research: Oceans **118**, 2961–2976.

Matsuda, H., Takenouchi, T. and Goldstein, J.S. (2006). The complete larval development of the pronghorn spiny lobster *Panulirus penicillatus* (Decapoda: Palinuridae) in culture. *Journal of Crustacean Biology* **26**, 579–600.

Matsuda, H. and Yamakawa, T. (2000). The complete development and morphological changes of larval *Panulirus longipes* (Decapoda, Palinuridae) under laboratory conditions. *Fisheries Science* **66**, 278–293.

McWilliam, P.S., Phillips, B.F. and Kelly, S. (1995). Phyllosoma larvae of scyllarus species (Decapoda, Scyllaridae) from the Shelf Waters of Australia. *Crustaceana* **68**, 537-566.

McWilliam, P.S. and Phillips, B.F. (1983). Phyllosoma larvae and other crustacean macrozooplankton associated with Eddy J, a warm-core eddy off south-eastern Australia. *Australian Journal of Marine Freshwater Research* **34**, 653–663.

Palero, F., Genis-Armero, R., Hall, M.R. and Clark, P.F. (2016). DNA barcoding the phyllosoma of *Scyllarides squammosus* (H. Milne Edwards, 1837) (Decapoda: Achelata: Scyllaridae). *Zootaxa* **4139**, 481–498.

Pecl, G., Frusher, S., Gardner, C., Haward, M., Hobday, A., Jennings, S., Nursey-Bray, M., Punt, A., Revill, H. and van Putten, I. (2009). *The east coast Tasmanian Rock Lobster Fishery: Vulnerability to climate change impacts and adaptation response options*. Report to the Department of Climate Change, Australia.

Pecl, G.T., Araújo, M.B., Bell, J.D., Blanchard, J., Bonebrake, T.C., Chen, I.-C., Clark, T.D., Colwell, R.K., Danielsen, F., Evengård, B., Falconi, L., Ferrier, S., Frusher, S., Garcia, R.A., Griffis, R.B., Hobday, A.J., Janion-Scheepers, C., Jarzyna, M.A., Jennings, S., Lenoir, J., Linnetved, H.I., Martin, V.Y., McCormack, P.C., McDonald, J., Mitchell, N.J., Mustonen, T., Pandolfi, J.M., Pettorelli, N., Popova, E., Robinson,

S.A., Scheffers, B.R., Shaw, J.D., Sorte, C.J.B., Strugnell, J.M., Sunday, J.M., Tuanmu, M.N., Vergés, A., Villanueva, C., Wernberg, T., Wapstra, E. and Williams, S.E. (2017). Biodiversity redistribution under climate change: Impacts on ecosystems and human well-being. *Science* **355**, eaai9214.

Phillips, B.F. and McWilliam, P.S. (1986) Phyllosoma and nisto stages of *Scyllarus martensii* Pfeffer (Decapoda, Scyllaridae) from the Gulf of Carpentaria, Australia. *Crustaceana* **51**, 133-154.

Pinsky, M.L., Worm, B., Fogarty, M.J., Sarmiento, J.L. and Levin S.A. (2013). Marine taxa track local climate velocities. *Science* **341**, 1239-1242.

Pitt, N.R., Poloczanska, E.S. and Hobday, A.J. (2010). Climate-driven range changes in Tasmanian intertidal fauna. *Marine and Freshwater Research* **61**, 963–970.

Poloczanska, E.S., Burrows, M.T., Brown, C.J., Molinos, J.G., Halpern, B.S., Hoegh-Guldberg, O., Kappel, C.V., Moore, P.J., Richardson, A.J., Schoeman, D.S. and Sydeman, W.J. (2016). Responses of marine organisms to climate change across oceans. *Frontiers in Marine Science* **3**, 1-21.

Prasad, R.R. and Tampi, P.R. (1959). On a collection of Palinurid phyllosomas from the Laccadive seas. *Journal of the Marine Biological Association of India* **1**, 143–165.

Ptacek, M., Sarver, S., Childress, M. and Herrnkind, W. (2001). Molecular phylogeny of the spiny lobster genus *Panulirus* (Decapoda: Palinuridae). *Marine Freshwater* **52**, 1037–47.

Ramos, J.E., Pecl, G.T., Moltschaniwskyj, N.A., Semmens, J.M., Souza, C.A. and Strugnell, J.M. (2018). Population genetic signatures of a climate change driven marine range extension. *Scientific Reports* **8**, 9558.

Ravago, R.G. and Juinio-Menez, A. (2002). Phylogenetic position of the striped-legged forms of *Panulirus longipes* (A. Milne-Edwards, 1868)(Decapoda, Palinuridae) inferred

from mitochondrial DNA sequences. *Crustaceana* **75**, 1047–1059.

Rees, A., Yearsley, G., Gowlett-Holmes, K. and Pogonoski, J. (1999). *Codes for Australian Aquatic Biota (Online Version)* [Online]. Available at: http://www.cmar.csiro.au/caab/.

Ridgway, K. and Hill, K. (2012). East Australian Current. In: *Marine Climate Change in Australia: Impacts and Adaptation. 2012 Report Card*. (Eds. ES Poloczanska, AJ Hobday and AJ Richardson). CSIRO, Canberra, Australia. 47–60.

Robinson, L.M., Gledhill, D.C., Moltschaniwskyj, N.A., Hobday, A.J., Frusher, S., Barrett, N., Stuart-Smith, J., and Pecl, G.T. (2015). Rapid assessment of an ocean warming hotspot reveals 'high' confidence in potential species' range extensions. *Global Environmental Change* **31**, 28–37.

Säwström, C., Beckley, L.E., Saunders, M.I., Thompson, P.A. and Waite, A.M. (2014). The zooplankton prey field for rock lobster phyllosoma larvae in relation to oceanographic features of the south-eastern Indian Ocean. *Journal of Plankton Research* **36**, 1003–1016.

Smith, S. and Simpson, R. (1991). Nearshore corals of the Coffs Harbour Region, mid north coast, New South Wales. *Wetlands (Australia)* **11**, 1–9.

Song, H., Buhay, J.E., Whiting, M.F. and Crandall, K.A. (2008). Many species in one: DNA barcoding overestimates the number of species when nuclear mitochondrial pseudogenes are coamplified. *Proceedings of the National Academy of Sciences* **105**, 13486–13491.

Sorte, C.J.B., Pandori, L.L.M., Cai, S. and Davis, K.A. (2018). Predicting persistence in benthic marine species with complex life cycles: linking dispersal dynamics to redistribution potential and thermal tolerance limits. *Marine Biology* **165**, 20.

Stuart-Smith, J., Pecl, G., Pender, A., Tracey, S., Villanueva, C. and Smith-Vaniz, W.F.

(2018). Southernmost records of two *Seriola* species in an Australian ocean-warming hotspot. *Marine Biodiversity,* 1–4.

Sun, C., Feng, M., Matear, R.J., Chamberlain, M.A., Craig, P., Ridgway, K.R. and Schiller, A. (2012). Marine downscaling of a future climate scenario for Australian boundary currents. *Journal of Climate* **25**, 2947–2962.

Sunday, J.M., Bates, A.E. and Dulvy, N.K. (2012). Thermal tolerance and the global redistribution of animals. *Nature Climate Change* **2**, 686–690.

Sunday, J.M., Pecl, G.T., Frusher, S., Hobday, A.J., Hill, N., Holbrook, N.J., Edgar, G.J., Stuart-Smith, R., Barrett, N., Wernberg, T., Watson, R.A., Smale, D.A., Fulton, E.A., Slawinski, D., Feng, M., Radford, B.T., Thompson, P.A. and Bates, A.E. (2015). Species traits and climate velocity explain geographic range shifts in an ocean-warming hotspot. *Ecology Letters* **18**, 944–953.

Suthers, I.M., Young, J.W., Baird, M.E., Roughan, M., Everett, J.D., Brassington, G.B., Byrne, M., Condie, S.A., Hartog, J.R., Hassler, C.S., Hobday, A.J., Holbrook, N.J., Malcolm, H.A., Oke, P.R., Thompson, P.A. and Ridgway, K. (2011). The strengthening East Australian Current, its eddies and biological effects — an introduction and overview. *Deep Sea Research Part II: Topical Studies in Oceanography* **58**, 538–546.

Syahailatua, A., Roughan, M. and Suthers, I.M. (2011). Characteristic ichthyoplankton taxa in the separation zone of the East Australian Current: larval assemblages as tracers of coastal mixing. *Deep-Sea Research Part II: Topical Studies in Oceanography* **58**, 678–690.

Tampi, P.R. and George, M.J. (1975). Phyllosoma larvae in the IIOE (1960-65) collections - systematics. *Mahasagar* **8**, 15–44.

Tranter, D.J., Tafe, D.J. and Sandland, R.L. (1983). Some zooplankton characteristics of

warm-core eddies shed by the East Australian Current, with particular reference to copepods. *Australian Journal of Marine Freshwater Research* **34**, 587–607.

Vergés, A., Steinberg, P.D., Hay, M.E., Poore, A.G.B., Campbell, A.H., Ballesteros, E., Heck Jr., K.L., Booth, D.J., Coleman, M.A., Feary, D.A., Figueira, W., Langlois, T., Marzinelli, E.M., Mizerek, T., Mumby, P.J., Nakamura, Y., Roughan, M., van Sebille, E., Gupta, A.S., Smale, D.A., Tomas, F., Wernberg, T., and Wilson, S.K. (2014). The tropicalization of temperate marine ecosystems: climate-mediated changes in herbivory and community phase shifts. *Proceedings of The Royal Society B* **281**, 20140846.

Wakabayashi, K., Yang, C.H., Shy, J.Y., He, C.H. and Chan, T.Y. (2017) Correct identification and redescription of the larval stages and early juveniles of the slipper lobster *Eduarctus martensii* (Pfeffer, 1881) (Decapoda:Scyllaridae). *Journal of Crustacean Biology* **37**, 204–219.

Wang, M., O'Rorke, R., Waite, A.M., Beckley, L.E., Thompson, P. and Jeffs, A.G. (2015). Condition of larvae of western rock lobster (*Panulirus cygnus*) in cyclonic and anticyclonic eddies of the Leeuwin Current off Western Australia. *Marine and Freshwater Research* **66**, 1158–1167.

Yang, C.H. and Chan, T.Y. (2010). A new slipper lobster of the genus *Galearctus* Holthuis, 2002 (Decapoda, Scyllaridae) from Taiwan and Japan. In: *Studies on Malacostraca. Lipke Bijdeley Holthuis Memorial Volume. Crustaceana Monographs*. (Eds C Fransen, S De Grave, and P Ng) Brill, Leiden. 735–745.

1.5 Supplementary Information

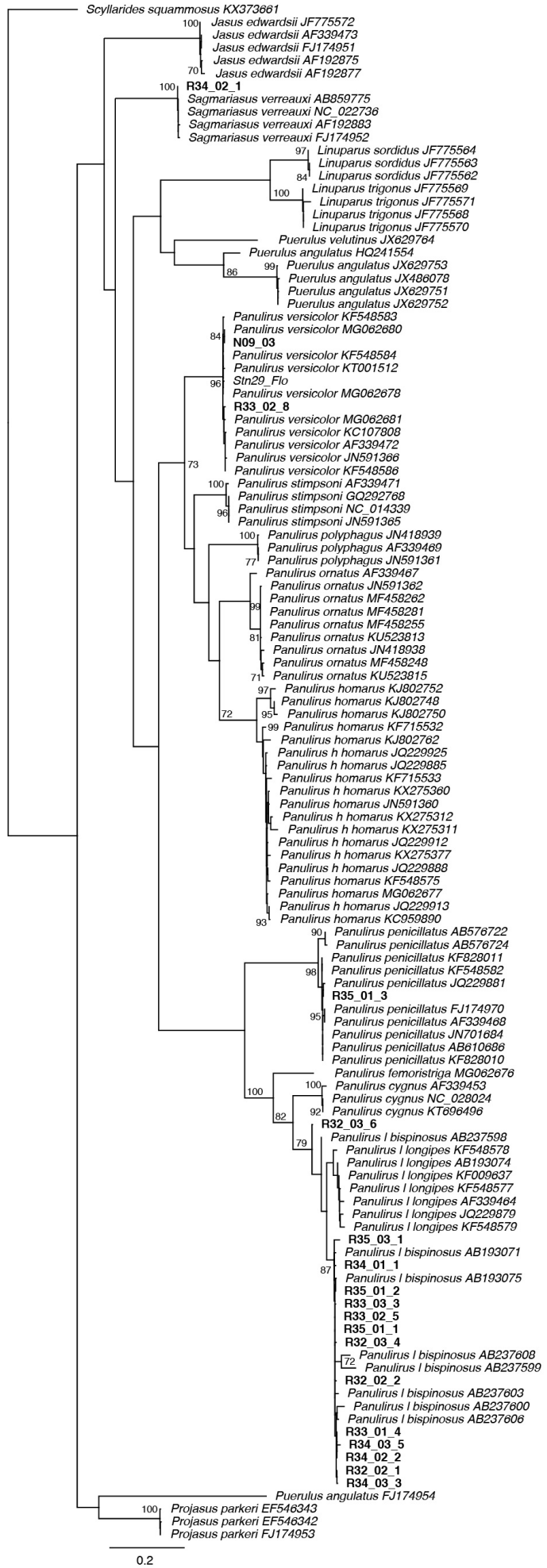

Fig. S1. A palinurid maximum-likelihood species identification tree using all available COI sequences or the 10 most divergent COI sequences as references. The tree was built with a HKY substitution model and *Scyllarides squammosus* as the outgroup. Collected samples are denoted by letter and number

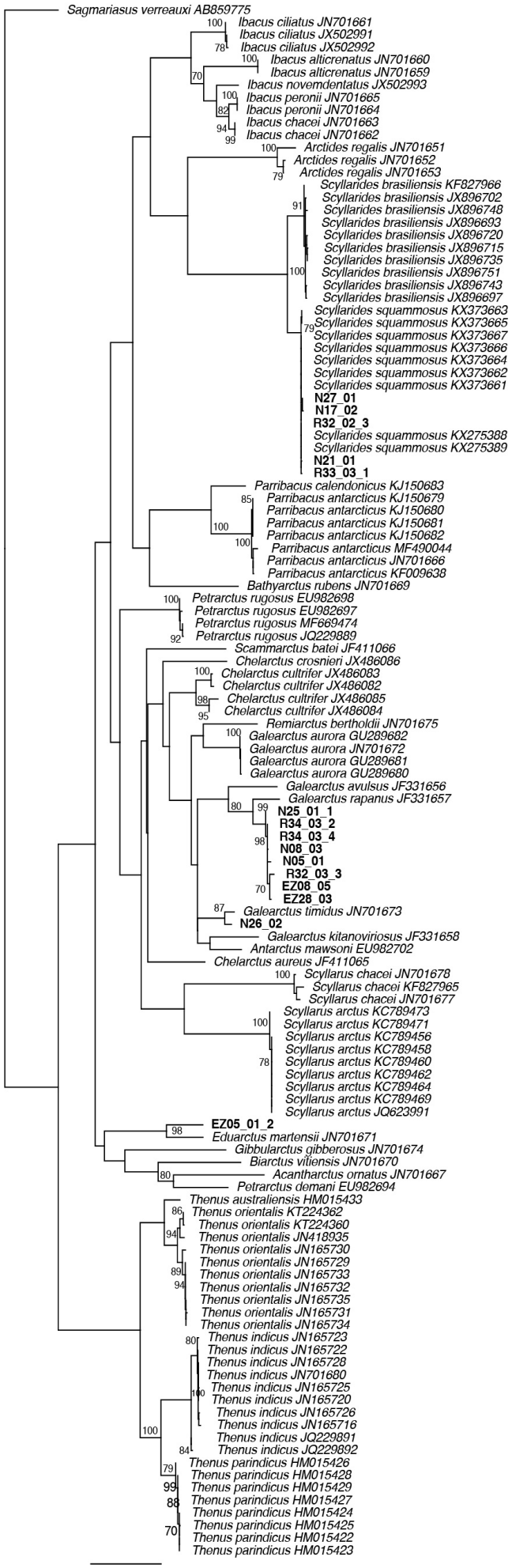

combinations. Node labels represent bootstrap values from 1000 replicates.

Fig. S2. A scyllarid maximum likelihood species identification tree using all available COI sequences or the 10 most divergent COI sequences as references. The tree was built with a HKY substitution model and *Sagmariasus verreauxi* as the outgroup. Collected

samples are denoted by letter and number combinations. Node labels represent bootstrap values from 1000 replicates.

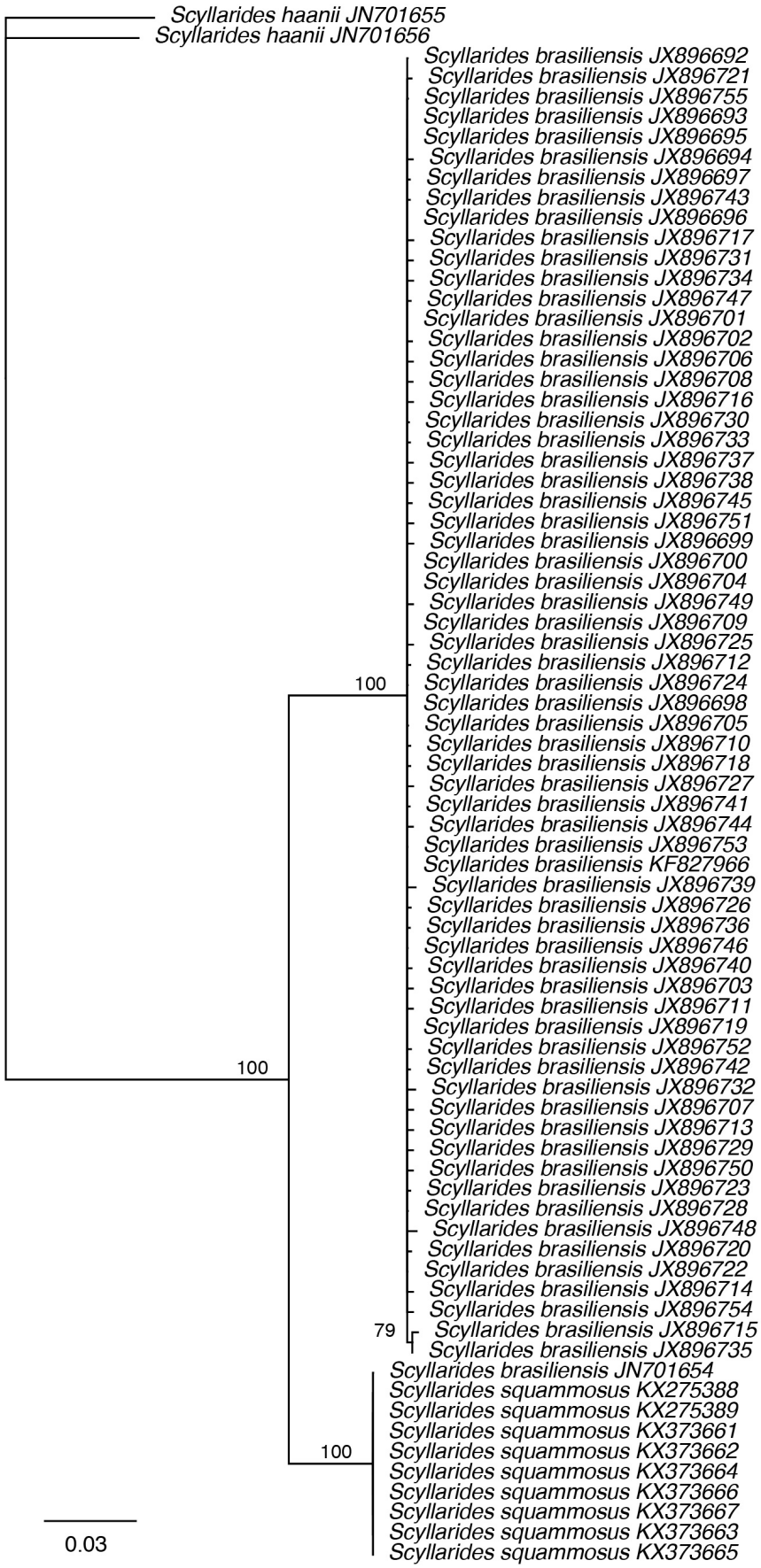
Scyllarides haanii JN701655
Scyllarides haanii JN701656
Scyllarides brasiliensis JX896692
Scyllarides brasiliensis JX896721
Scyllarides brasiliensis JX896755
Scyllarides brasiliensis JX896693
Scyllarides brasiliensis JX896695
Scyllarides brasiliensis JX896694
Scyllarides brasiliensis JX896697
Scyllarides brasiliensis JX896743
Scyllarides brasiliensis JX896696
Scyllarides brasiliensis JX896717
Scyllarides brasiliensis JX896731
Scyllarides brasiliensis JX896734
Scyllarides brasiliensis JX896747
Scyllarides brasiliensis JX896701
Scyllarides brasiliensis JX896702
Scyllarides brasiliensis JX896706
Scyllarides brasiliensis JX896708
Scyllarides brasiliensis JX896716
Scyllarides brasiliensis JX896730
Scyllarides brasiliensis JX896733
Scyllarides brasiliensis JX896737
Scyllarides brasiliensis JX896738
Scyllarides brasiliensis JX896745
Scyllarides brasiliensis JX896751
Scyllarides brasiliensis JX896699
Scyllarides brasiliensis JX896700
Scyllarides brasiliensis JX896704
Scyllarides brasiliensis JX896749
Scyllarides brasiliensis JX896709
Scyllarides brasiliensis JX896725
Scyllarides brasiliensis JX896712
Scyllarides brasiliensis JX896724
Scyllarides brasiliensis JX896698
Scyllarides brasiliensis JX896705
Scyllarides brasiliensis JX896710
Scyllarides brasiliensis JX896718
Scyllarides brasiliensis JX896727
Scyllarides brasiliensis JX896741
Scyllarides brasiliensis JX896744
Scyllarides brasiliensis JX896753
Scyllarides brasiliensis KF827966
Scyllarides brasiliensis JX896739
Scyllarides brasiliensis JX896726
Scyllarides brasiliensis JX896736
Scyllarides brasiliensis JX896746
Scyllarides brasiliensis JX896740
Scyllarides brasiliensis JX896703
Scyllarides brasiliensis JX896711
Scyllarides brasiliensis JX896719
Scyllarides brasiliensis JX896752
Scyllarides brasiliensis JX896742
Scyllarides brasiliensis JX896732
Scyllarides brasiliensis JX896707
Scyllarides brasiliensis JX896713
Scyllarides brasiliensis JX896729
Scyllarides brasiliensis JX896750
Scyllarides brasiliensis JX896723
Scyllarides brasiliensis JX896728
Scyllarides brasiliensis JX896748
Scyllarides brasiliensis JX896720
Scyllarides brasiliensis JX896722
Scyllarides brasiliensis JX896714
Scyllarides brasiliensis JX896754
Scyllarides brasiliensis JX896715
Scyllarides brasiliensis JX896735
Scyllarides brasiliensis JN701654
Scyllarides squammosus KX275388
Scyllarides squammosus KX275389
Scyllarides squammosus KX373661
Scyllarides squammosus KX373662
Scyllarides squammosus KX373664
Scyllarides squammosus KX373666
Scyllarides squammosus KX373667
Scyllarides squammosus KX373663
Scyllarides squammosus KX373665
100
100
100
79
0.03

Fig. S3. A Neighbor Joining tree using all COI sequences available in GenBank for *Scyllarides brasiliensis*, *Scyllarides hanii* and *Scyllarides squammosus*. Note that JN701654 groups within the *S. squammosus* clade. Node labels represent consensus support over 1000 bootstraps.